Cell

A Molecular Mousetrap Determines Polarity of Termination of DNA Replication in *E. coli*

Mark D. Mulcair,[1] Patrick M. Schaeffer,[1] Aaron J. Oakley,[1] Hannah F. Cross,[2] Cameron Neylon,[2] Thomas M. Hill,[3] and Nicholas E. Dixon[1,*]
[1] Research School of Chemistry, Australian National University, Canberra, ACT 0200, Australia
[2] School of Chemistry, University of Southampton, SO17 1BJ, UK
[3] Department of Microbiology and Immunology, School of Medicine and Health Sciences, University of North Dakota, Grand Forks, ND 58202, USA
*Contact: dixon@rsc.anu.edu.au
DOI 10.1016/j.cell.2006.04.040

SUMMARY

During chromosome synthesis in *Escherichia coli*, replication forks are blocked by Tus bound *Ter* sites on approach from one direction but not the other. To study the basis of this polarity, we measured the rates of dissociation of Tus from forked *TerB* oligonucleotides, such as would be produced by the replicative DnaB helicase at both the fork-blocking (nonpermissive) and permissive ends of the *Ter* site. Strand separation of a few nucleotides at the permissive end was sufficient to force rapid dissociation of Tus to allow fork progression. In contrast, strand separation extending to and including the strictly conserved G-C(6) base pair at the nonpermissive end led to formation of a stable locked complex. Lock formation specifically requires the cytosine residue, C(6). The crystal structure of the locked complex showed that C(6) moves 14 Å from its normal position to bind in a cytosine-specific pocket on the surface of Tus.

INTRODUCTION

In most bacterial species, chromosomal DNA replication initiates at a unique origin (*oriC* in *Escherichia coli*), and it proceeds bidirectionally until the two replication forks meet in the terminus region located opposite the origin (Figure 1A). The *E. coli* terminus contains ten 23 bp *Ter* sites (*TerA–J*) arranged in two oppositely oriented groups of five (Coskun-Ari and Hill, 1997). Each of the *Ter* sites binds Tus, the 36 kDa terminator protein (Hill et al., 1989; Hidaka et al., 1989; Hill, 1992; Kamada et al., 1996; reviewed in Neylon et al., 2005). Thus the first of the two forks to arrive in the terminus region encounters the same face of Tus bound at each of the first series of *Ter* sites, termed the permissive face. It apparently displaces the bound Tus and passes through to the second series, where it now encounters a nonpermissive face, and its progress is blocked: the fork is trapped between oppositely oriented *Ter* sites (Hill et al., 1987; Hill, 1992).

Since the ten *Ter* sites have no inverted symmetry of sequence or direct repeats (Figure 1B), and Tus is a monomeric protein that forms a simple 1:1 complex with them (Coskun-Ari et al., 1994), this evident polarity of fork arrest cannot be due to Tus acting as a simple thermodynamic clamp. Moreover, despite knowledge of the crystal structure of a Tus-*TerA* complex (Kamada et al., 1996) and extensive work on the process of replication fork arrest and the stability of complexes of Tus with variant *Ter* sites, there has been no satisfactory explanation of the mechanism that determines polarity of the Tus-*Ter* block (reviewed by Neylon et al., 2005). This mechanism is resolved in the present work.

The X-ray crystal structure of the Tus-*TerA* complex showed that many of the conserved residues among the various *Ter* sites make base-specific contacts with the protein (Kamada et al., 1996; Neylon et al., 2005). The dissociation constant (K_D) of the Tus-*TerB* complex was reported to be 0.3 pM in 0.15 M potassium glutamate, and the half-life of the complex was 550 min (Gottlieb et al., 1992). This is therefore the most stable complex known of a monomeric, sequence-specific, DNA binding protein with its double-stranded recognition sequence. As expected for a complex in which many interactions are electrostatic (Kamada et al., 1996), binding is strongly dependent on ionic strength, with the value of K_D rising to about 1 nM and the half-life decreasing to about 2 min in a buffer containing 0.25 M KCl, as assessed by surface plasmon resonance (SPR) studies (Neylon et al., 2000).

Complexity beyond simple DNA binding in determining the polarity of fork arrest is suggested by identification of mutants of *TerB* that bind Tus as strongly as the wild-type but that are defective in replication fork arrest in vivo (Coskun-Ari and Hill, 1997) and mutants of Tus that are more defective in fork arrest than DNA binding

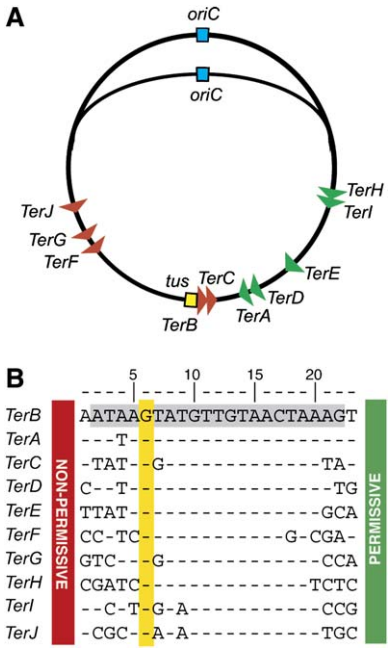

Figure 1. Polarity of Replication Termination in *E. coli*

(A) Replication initiates at *oriC* and proceeds bidirectionally. The clockwise-moving replication fork passes through the *Ter* sites shown in green but is arrested at sites in red. The opposite is true for the fork moving in the counterclockwise direction. The yellow box indicates the location of the *tus* gene.

(B) Sequences of the ten *Ter* sites. Forks arriving at the nonpermissive face are blocked, while those entering from the permissive face pass through. The 21 bp *TerB* sequence used in SPR studies is highlighted in gray and the strictly conserved G-C(6) base pair in yellow.

(Skokotas et al., 1995; Henderson et al., 2001). Residues specifically implicated in this behavior are the G-C(6) base pair of *Ter* (Figure 1B) and the side chain of Glu49 of Tus.

Alternate mechanisms for determination of polarity in this system have been discussed in detail by Neylon et al. (2005). The major replicative helicase (DnaB) is the first replisomal protein at a replication fork to encounter the Tus-*Ter* complex (Schaeffer et al., 2005), and binding of Tus has been known for some time to compromise unwinding of *Ter* DNA by DnaB in vitro in a polar fashion (Lee et al., 1989; Khatri et al., 1989). A direct physical interaction between Tus and DnaB at the nonpermissive face that prevents unwinding of *Ter* is a potential mechanism to enforce polarity, and there is experimental support for this (Mulugu et al., 2001). However, a major difficulty with this mechanism is that the Tus-*Ter* complex seems to exhibit polarity in inhibition of strand separation by a variety of DNA helicases, including some that move on their single-stranded DNA tracks in the 5′–3′ direction (such as DnaB) and those that have 3′–5′ polarity (e.g., *E. coli* Rep, PriA, UvrD, and SV40 virus large T antigen) (Lee et al., 1989; Khatri et al., 1989; Bedrosian and Bastia, 1991; Lee and Kornberg, 1992; Hidaka et al., 1992; Sahoo et al., 1995). Moreover, transcription by *E. coli* RNA polymerase is also reported to be blocked in a polar manner (Sahoo et al., 1995; Mohanty et al., 1998).

We found previously that the kinetics of interaction of Tus with *TerB* were affected differently by mutations in Tus, depending on their location at the permissive or the nonpermissive face of the complex, and these data suggested that dissociation of Tus occurs in a stepwise manner (Neylon et al., 2000). Polarity could then be explained by the existence of a different series of elementary steps in dissociation of the complex when the helicase approaches from one face as opposed to the other (Neylon et al., 2005).

This led to a more precise definition of this hypothesis, considered here: That approach of DnaB, at the forefront of the replisome, to a Tus-*Ter* complex engineers a structure in DNA that differentially affects dissociation of Tus depending on the direction of approach. The simplest DNA structure engineered by a helicase is forked duplex DNA, and a simple way to test the hypothesis was to measure the rates of dissociation of Tus from forked variants of *TerB* that mimic structures that would be produced by helicase action. Here, we first show that the rates of dissociation of Tus from forked *TerB* oligonucleotides are indeed profoundly different, depending on whether the fork is at one end of *TerB* or the other. In particular, forks that expose the strictly conserved G-C(6) base pair at the nonpermissive face produce a complex in which Tus is locked onto the DNA: It dissociates about 40-fold more slowly than from wild-type *TerB*. We trace this locking behavior to a single nucleotide base (C6) of *Ter*, which we propose forms a new contact with a cryptic cytosine-specific, single-stranded DNA binding site on the surface of Tus. This site is then identified in an X-ray crystal structure of Tus in complex with an appropriate forked duplex version of *Ter*.

Finally, we address the question of what may happen when the later-arriving, oppositely moving replisome approaches the first replisome stalled at the Tus-*Ter* complex: we show that strand separation at the permissive face can unlock the first complex, displacing Tus to allow replication of the remaining double-stranded DNA at the terminus. These studies thus provide simple and elegant explanations of many of the unresolved questions regarding the mechanism of replication fork arrest at Tus bound *Ter* sites in the final stages of chromosomal DNA replication. In addition, they reveal an unprecedented stable interaction between a monomeric DNA binding protein and a particular forked DNA structure, which might be exploited in practical ways.

RESULTS AND DISCUSSION

The kinetics and thermodynamics of interaction of Tus with *TerB* and its forked versions were studied by SPR using a Biacore instrument at 20°C in a buffer at pH 7.5 containing 250 mM KCl; 21 nucleotide 5′-biotinylated *TerB* oligonucleotides were immobilized through an abasic spacer to streptavidin-coated Biacore chip surfaces (Neylon et al., 2000). Each of the strands of *TerB* was

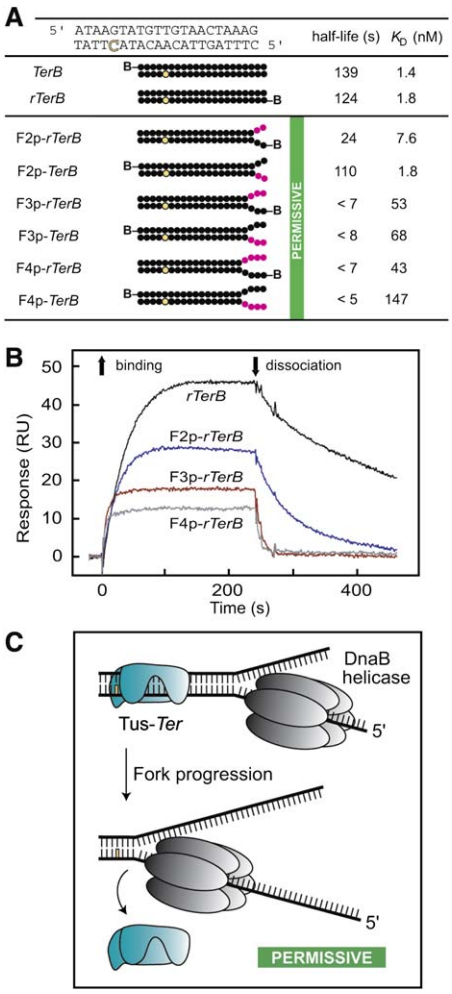

Figure 2. Extension of Forks at the Permissive End of *TerB* Results in Progressively More Rapid Dissociation of Tus

(A) Half-lives and dissociation constants (K_D) of complexes of Tus with *TerB* oligonucleotides that have forks at the permissive end, as measured by SPR in buffer containing 0.25 M KCl. Base substitutions that replace the natural *TerB* sequence are shown in magenta, and the C(6) residue is in yellow. "B–" denotes the strand that was modified with a 5′-biotinylated ten residue abasic spacer. Sequences of oligonucleotides and complete SPR data, including estimates of errors, are given in Figure S1.

(B) Representative Biacore sensorgrams with different oligonucleotides are shown for binding of 20 nM His_6-Tus. Data were normalized on the basis of the measured maximum response at saturating [Tus] (~50 response units).

(C) Model for dissociation of Tus following DnaB-mediated strand separation at the permissive face of the Tus-*Ter* complex.

immobilized separately, and the other (hybridized) strand contained noncomplementary regions (e.g., as shown in Figure 2A). We could thus examine dissociation of Tus from *TerB* sites containing noncomplementary mutated regions of various lengths on both strands at each end. As observed previously (Neylon et al., 2000), the interaction of Tus with *TerB* is a well-behaved interaction for study by SPR. Dissociation generally followed a first-order rate law; half-lives and values of K_D for the wild-type complex in both orientations (*TerB* and *rTerB*) are given in Figure 2A (complete kinetic and thermodynamic data, including estimates of error limits in all measurements, and sequences of these and all other oligonucleotides are given in Figure S1 in the Supplemental Data available with this article online). The data for *TerB* and *rTerB* indicate that the orientation of the wild-type duplex with respect to the surface has little effect on binding parameters. Values of K_D were 1–2 nM; use of 250 mM KCl in the buffer brings parameters into a range reliably quantifiable by SPR (Neylon et al., 2000).

Strand Separation at the Permissive Face of *TerB* Leads to Rapid Dissociation of Tus

As the forked region was progressively extended at the permissive end of *TerB*, dissociation rates became progressively faster, and it mattered little which strand was mutated (Figures 2A and 2B) or if either of them was removed completely (Figure S1). It is clear that strand separation even as far as A-T(20) of *TerB* would lead to rapid dissociation of Tus (Figure 2A, oligonucleotides F3p-*TerB* and F3p-*rTerB*), resulting in unimpeded progression of the replisome through *Ter* (Figure 2C). The data are thus consistent with removal of Tus due to the progressive loss of protein-DNA contacts during strand separation by the helicase at the permissive end of *Ter*.

Tus Locks onto Strand-Separated Duplexes at the Nonpermissive Face

The situation was different with single-stranded regions at the nonpermissive end. A 5- to 7-fold increase in K_D was observed when the mismatched regions were three or four nucleotides long, with dissociation rates similar to those with wild-type *TerB* regardless of which strand was mutated (Figures 3A and 3B). However, strand specificity became dramatically obvious when the forked region extended to the G-C(6) base pair. When the strand containing C(6) was mutated (the bottom strand in Figure 3A; oligonucleotide F5n-*TerB*), Tus dissociated about twice as rapidly as from *TerB* (Figures 3A and 3C), and K_D increased almost 30-fold. On the other hand, mutation of the top strand (F5n-*rTerB*) resulted in Tus being firmly locked onto the forked *TerB* (Figures 3A–3C): Tus dissociated about 40-fold more slowly than from *TerB*, and K_D was about 3-fold lower. Although extension of the fork to include T-A(7) (F6n-*rTerB*) resulted in a similarly locked behavior, its further lengthening to A-T(8) (F7n-*rTerB*) resulted in poorer binding because of a slower association rate (Figures 3A and S1).

It is clear therefore that strand separation by a helicase approaching from the nonpermissive face of the Tus-*Ter* complex would lead to a locked complex that is even more stable than the regular complex with fully duplex *TerB*, while at the permissive face helicase action would simply promote dissociation of Tus. These observations provide an adequate explanation of the polarity observed in replication termination.

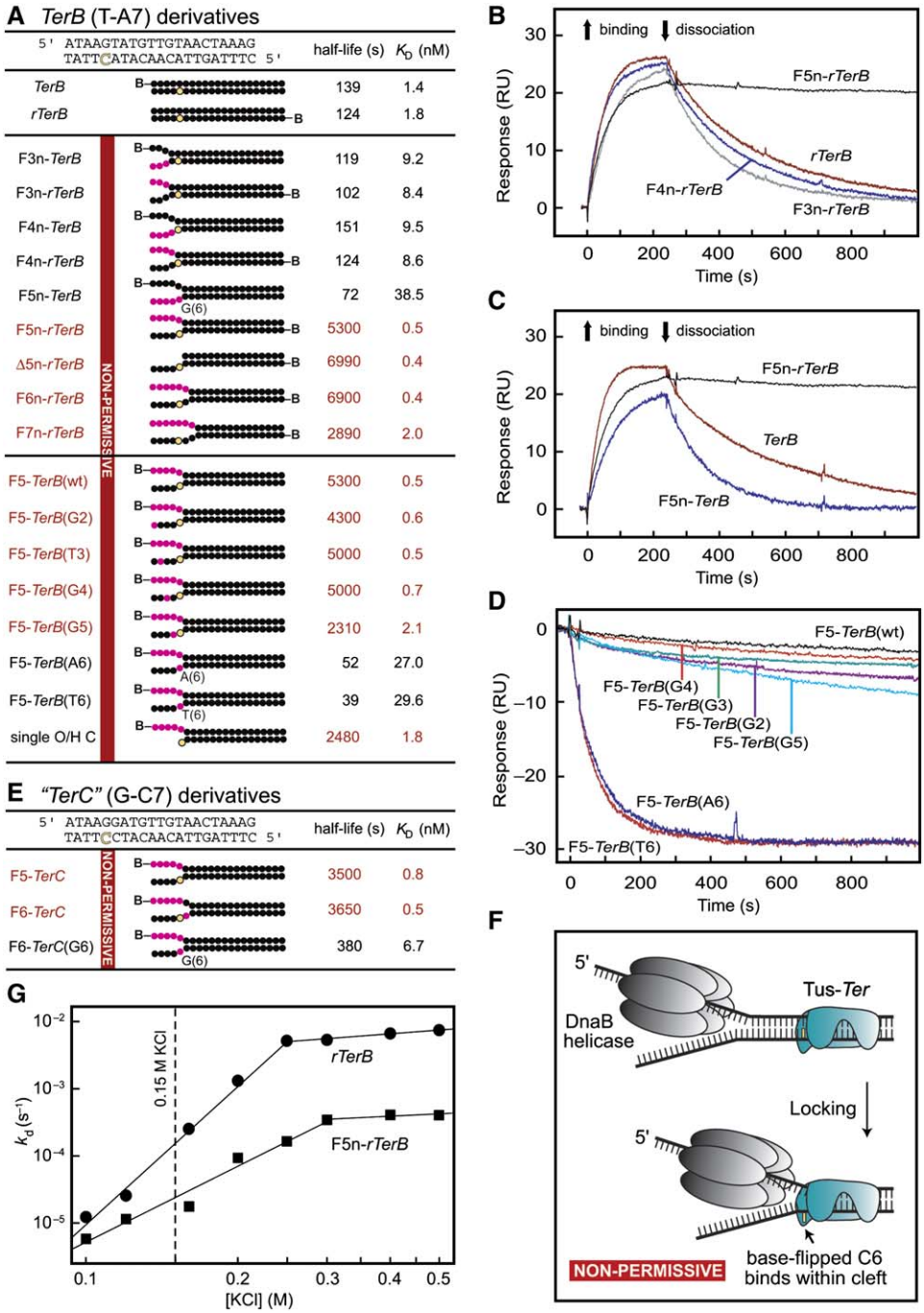

Figure 3. A Molecular Mousetrap Determines Polarity of Replication Fork Arrest

(A) Dissociation of Tus from complexes with *TerB* oligonucleotides forked at the nonpermissive end, measured by SPR. Data for the *TerB* variants that show the locked behavior are in red. Color coding is otherwise as in Figure 2A.

(B) The locked complex forms when the fork extends far enough to expose C(6) (in F5n-*rTerB*). Representative Biacore sensorgrams show His_6-Tus (10 nM) interaction with wild-type and forked *TerB* sequences.

(C) Strand specificity of locking behavior at the nonpermissive end of *TerB* (10 nM Tus).

(D) A single nucleotide, C(6) of *TerB*, is responsible for formation of the locked species: effect of base substitution on dissociation of Tus from forked *TerB* sequences. His_6-Tus was bound at a saturating concentration (100 nM) to forked *TerB* species containing mutations in T(2) to C(6). Tus formed a lock on all except those where C(6) had been mutated to adenine or thymine (or guanosine, see F5n-*TerB* in [C]).

(E) Half-lives and dissociation constants of Tus complexes with *Ter* oligonucleotides with T-A(7) of *TerB* substituted by G-C as in *TerC*.

A Single Nucleotide Determines Polarity of Fork Arrest

It is clear that the strictly conserved C(6) base on the bottom strand of the *TerB* sequence in Figure 3A must not be base-paired to lock the complex. Some further experiments verified this. The locking behavior still occurred when the first five residues of the mutant strand in F5n-*rTerB* were completely removed (Δ5n-*rTerB*; Figure 3A), indicating that a forked structure is not required and systematic mutagenesis of each of the first five residues of the wild-type strand of F5n-*rTerB* showed that mutagenesis of C(6), and only C(6), abrogated the locking behavior of the complex (Figures 3A, 3C, and 3D). Indeed, complete removal of the first four residues on the 3′ strand, leaving only C(6), still resulted in formation of a locked species ("single O/H C," Figure 3A). The unpaired C(6) residue is thus necessary and sufficient for lock formation.

The T-A(7) base pair in *TerB* is not conserved, being replaced by G-C in *TerC* and two other *Ter* sites (Figure 1B). Its mutagenesis resulted in only small effects on the strength of the Tus-*TerB* interaction or in vivo fork arrest activity (Coskun-Ari and Hill, 1997). Data in Figure 3E show that changing T-A(7) to G-C has very little effect on formation or stability of the locked species and that substitution of C(6) by G again results in loss of the locking behavior.

These data indicate that a molecular mousetrap operates during replication fork arrest at the nonpermissive face of Tus-*Ter* (Figure 3F). The trap is set by the binding of Tus to the *Ter* site, and it is sprung by strand separation by DnaB at the forefront of the approaching replisome. This results in the flipping of the C(6) residue out of the double helix by rotation of the phosphodiester backbone and its base-specific binding in a cryptic cytosine-specific binding pocket in or near the DNA binding channel of Tus. Other contacts of Tus with the displaced strand may occur, but they are not sequence specific.

Base-flipping processes that bear some similarity to this occur in DNA modification and repair enzymes like DNA *N*-glycosylases, apurinic endonucleases, and DNA methyltransferases (Cheng and Roberts, 2001). This mechanism explains the observation that mutagenesis of the G-C(6) base pair of *TerB* compromises fork arrest without severely affecting Tus binding (Coskun-Ari and Hill, 1997) and the strict conservation of this base pair in all *Ter* sites (Figure 1B). Specific physical interaction of DnaB with Tus is not precluded but would appear to be unnecessary. Several further experiments were carried out to study aspects of this model.

Formation of the Tus-*Ter* Lock is Masked in Potassium Glutamate Buffers

We anticipated that Tus would dissociate very slowly from oligonucleotides that expose C(6) at the nonpermissive end in 200 mM potassium glutamate buffer at 25°C, conditions that have been used in many earlier studies of the Tus-*Ter* interaction (e.g., see Skokotas et al., 1995; Henderson et al., 2001); the half-life of the wild-type Tus-*TerB* complex is 150 min in this buffer. Accordingly, measurements of dissociation of Tus from ^{32}P-labeled *TerB* and partial-duplex *TerB* derivatives (Table 1) in solution were made using the conventional filter binding assay. Complexes with Tus were challenged with excess unlabeled *TerB* oligonucleotide, and samples were filtered at various times to determine the proportion of protein bound ^{32}P remaining. Dissociation of Tus generally followed a first-order rate law; half-lives of the complexes are given in Table 1. It is apparent that dissociation half-lives in glutamate buffer were much more similar for the wild-type *TerB* oligonucleotide and those that expose C(6), indicating that the locked conformation of the DNA either no longer forms under these conditions or, more likely, that its dissociation from Tus occurs at a similar rate as from wild-type *TerB*, i.e., existence of the lock is masked by the higher stability of the wild-type complex.

Ionic Strength Dependence of the Tus-*Ter* Interactions

These observations prompted examination of the effects of ionic strength on dissociation rate constants (k_d) as measured by SPR (Figure 3G). At high ionic strength, a large difference in k_d was observed for F5n-*rTerB* cf. *rTerB*, with little dependence on ionic strength. At low ionic strength, the two lines in Figure 3G have a steeper slope and converge. The slopes of lines in such *log/log* plots are directly related to the numbers of ionic contacts that need to be disrupted during the rate-determining step in the dissociation of a protein from a DNA complex (Record et al., 1991). These data therefore offer further support for a stepwise mechanism for dissociation of Tus from both *TerB* (Neylon et al., 2000) and the forked species, and they show that the rate-determining step in each process changes abruptly with ionic strength. With both oligonucleotides, the slowest step in dissociation at high ionic strength involves loss of a single (or few) ionic interaction(s), while at low ionic strength the rate-determining step requires disruption of a much larger number of such interactions. The slowest step in dissociation of Tus from the locked complex at higher salt concentrations is likely to be removal of the C(6) base from its binding pocket, while for the wild-type complex, it is the breakage of a particular but undetermined site-specific interaction. At a physiological ionic strength corresponding to 150 mM KCl, the half-lives for the wild-type and locked complexes were still very different, being about 80 and 490 min, respectively (Figure 3G). Thus, the more stable locked

(F) Mousetrap model for fork arrest at the nonpermissive face. The trap is set by helicase action and sprung by base-flipping of C(6) into a binding site on the surface of Tus, resulting in a locked complex.

(G) Salt dependence of dissociation rate constants (k_d) at 20°C. The slopes of the least-squares fitted lines (*log/log* scales) were 6.8 ± 0.4 and 0.60 ± 0.08 for *rTerB* at low and high [KCl], respectively. Corresponding values for F5n-*rTerB* were 3.4 ± 0.3 and 0.32 ± 0.19.

Table 1. Half-lives for Dissociation of Tus-*Ter* Complexes in 200 mM Potassium Glutamate

Oligonucleotide[a]	Half-life (min)[b]
wt *TerB* 5'-AATAAGTATGTTGTAACTAAAGTGGATCAATTCATAA TTATTCATACAACATTGATTTCACCTAGTTAAGTATT-5'	150 ± 6
TerB_lock 5'-GGGGGCTATGTTGTAACTAAAGTGGATCAATTCATAA TTATTCATACAACATTGATTTCACCTAGTTAAGTATT-5'	131 ± 7
TerB_OH/C 5'-TATGTTGTAACTAAAGTGGATCAATTCATAAAATAAG CATACAACATTGATTTCACCTAGTTAAGTATTTTATTC-5'	205 ± 8

[a] The core *TerB* sequences are overlined.
[b] Average of three independent experiments (± SEM), using a competition filter binding assay in KG_{200} buffer at 25°C (Skokotas et al., 1995).

species would be expected to be generated by the action of DnaB under cellular conditions.

Tus Maintains Base-Specific Contacts in the Locked Complex

Duggan et al. (1996) showed that substitution of 5-bromo- or 5-iodo-deoxyuridine (IdU or BrdU) for thymidine at particular positions in *TerB* has a large stabilizing effect on its complex with Tus, presumably due to the presence of polarizable groups in pockets in the protein that accommodate the 5-methyl groups of thymidine. To verify that the structure of the locked species maintains these specific contacts, we examined the interaction of Tus with oligonucleotides simultaneously substituted at the T(8) and T(19) positions with IdU or BrdU. These substitutions had similar effects on the kinetics and thermodynamic parameters describing Tus interactions with both *TerB* and forked oligonucleotides (Figure 4A), suggesting that Tus maintains specific contacts with nucleotide bases of *TerB* at positions between A-T(8) and A-T(19) when the lock forms, and that the structure of the locked complex is similar to that of the wild-type complex in the central region and at the permissive face.

C(6) Base-Flipping Does Not Explain Lock Formation

Next we tested whether simple flipping of the C(6) base into a site lining the DNA binding channel of Tus could account for the locking behavior. We reasoned that base-flipping should occur readily with *TerB* oligonucleotides containing just a few unpaired bases around and including C(6), resulting in pronounced stabilization of their complexes with Tus. We used an extended version of *TerB* to ensure that the mismatched oligonucleotide strands remained hybridized at both ends while bound on the SPR chip. The binding and dissociation kinetics of Tus to wild-type *TerB* were unaffected by its extension to 37 bp (Figure 4B). The effects on dissociation rates of introducing mismatches at and around C(6) were rather modest until the unpaired region extended at least to five base pairs including A-T(3) to A-T(7) of *TerB* (Figure 4B). This suggested that although the only site-specific contact required for lock formation is with C(6), the presence of restrained regions of double-stranded DNA beyond the limits of the complex is inhibitory. This is inconsistent with a simple base-flipping mechanism. The X-ray structure of the locked complex explains these observations.

Crystal Structure of the Tus-*Ter* Lock

Crystals of Tus in complex with a forked oligonucleotide that resembles the truncated *TerA* oligonucleotide used by Kamada et al. (1996) for the wild-type complex were grown under slightly different conditions. In particular, inclusion of sodium iodide in the crystallization buffer improved crystallization, and progressive dehydration with increasing concentrations of PEG 3350 improved the quality of X-ray diffraction patterns. The structure was solved by molecular replacement, using the Tus-*TerA* structure as a starting model, to similar resolution (2.7 Å). Data collection and refinement statistics are given in Table S1. The initial model (R factor 43.5, R_{free} 41.23%) was improved by rigid body and positional refinement (R factor 43.07, R_{free} 40.92%). It was clear from the initial $2F_o-F_c$ and F_o-F_c electron density maps that the DNA structure at the nonpermissive face of the Tus-*Ter* complex no longer adopted a regular double-stranded structure. The maps revealed new density near Ile79, His144 and Phe140 of Tus (Figure 5A). Peaks in the F_o-F_c map of height 7.5 and 5.5 σ corresponded to the C(6) and adjacent A(7) bases. Additional spherical electron density located at crystal-contact positions were interpreted as iodide ions. After four rounds of model building and refinement, the R factor and R_{free} were 21.9% and 30.3%, respectively. The final model contains the altered DNA structure, residues 5–309 of Tus, 27 water molecules, and 3 iodide ions.

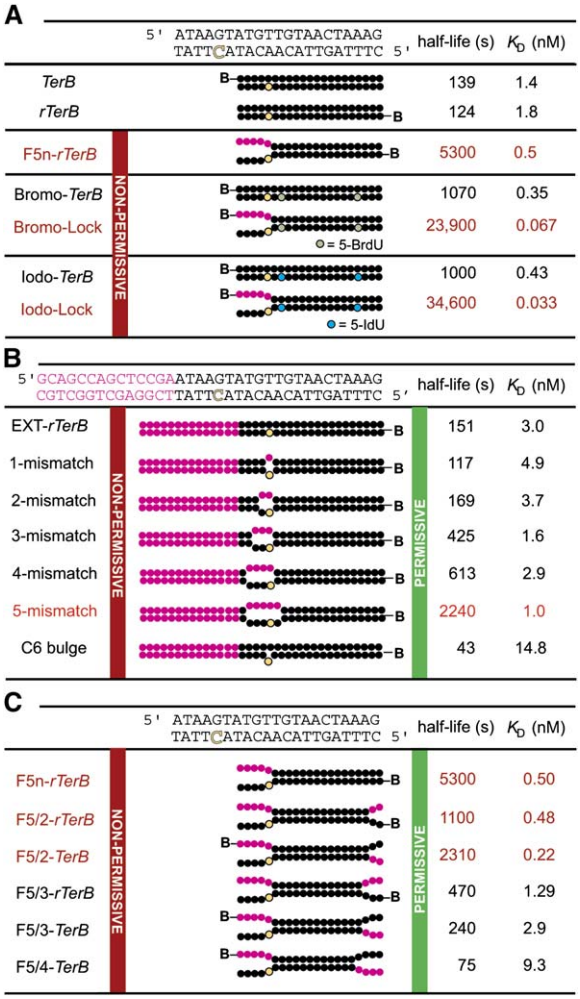

Figure 4. Further Properties of the Tus-*Ter* Lock

Half-lives and dissociation constants of Tus-*TerB* complexes. The diagram is color coded as in Figure 2A.

(A) The locked complex has many interactions in common with the complex of Tus with native *TerB* since substitution of T(8) and T(19) of *TerB* with 5-bromo- or 5-iodo-dUMP stabilize Tus complexes with duplex *TerB* and the lock to similar extents.

(B) An extensive single-stranded bubble, as in oligonucleotide "5-mismatch," is required to form the lock structure, suggesting it does not simply require flipping of the C(6) base.

(C) Unlocking of the Tus-*Ter* lock on approach of a second replisome to the permissive face. Presented are data for complexes of Tus with *TerB* oligonucleotides forked at both the permissive and nonpermissive ends.

Structure of *Ter* DNA in the Tus-*Ter* Lock

The structure contains all residues on both *Ter* DNA strands at the permissive end of the locked complex except for the unpaired T(20) at the 5′ end and A(19) at the 3′ end; these residues were also disordered in the earlier structure (Kamada et al., 1996). Nucleotides in both strands extending from T-A(18) as far as the A-T(8) base pair occupy positions essentially identical to those in the Tus complex with *TerA*, and they interact with the same residues in the protein (Figures 5B and 5C). However, residues in the unpaired region at the nonpermissive face either occupy radically different positions or show no electron density at this resolution. In particular, we were able to locate only the phosphate of T(5), the last residue at the 3′ end, and we were unable to detect the three unpaired nucleotides at the 5′ end of the other strand.

Consistent with predictions from the biochemical data, the major differences between the structures of the DNA ligands involve residues that include C(6) at the nonpermissive face (Figure 5). The C(6) base is flipped out of and away from the duplex to bind in a pocket near helix α4 of Tus, centered about 14 Å away from its position in the duplex DNA structure (Figure 5D). All three hydrogen bonding donors/acceptors of the C(6) base form hydrogen bonds with the protein: O2' with the peptide NH of Gly149, N3 with the imidazole $N^{\delta}H$ of His144, and the 4-NH_2 group with the peptide carbonyl of Leu150 (Figure 5E). The C(6) base ring is otherwise sandwiched in a hydrophobic pocket between the side chains of Ile79 and Phe140. In order for C(6) to reach its binding pocket, the T-A(7) base pair of the ligand DNA is also disrupted in the complex, with A(7) also moved out of the helix to stack on the opposite face of the phenyl ring of Phe140. It appears to make no base-specific contacts, consistent with the lack of sequence conservation at this position in known *Ter* sites (Figure 1B). The fact that oligonucleotides F6n-*rTerB* and F6-*TerC* (Figures 3A and 3E), which contain a mispair at position 7, form locked structures that dissociate as slowly as the corresponding F5n-*rTerB* and F5-*TerC* complexes is consistent with the observed melting of the T-A(7) base pair in the structure.

Structure of Tus in the Tus-*Ter* Lock

The overall structure of Tus in the locked complex is very similar to that in the Tus-*TerA* complex (Figures 5B and 5C), except for some conformational differences in the loops that normally interact with the 5′ strand at the nonpermissive face; residues in these loops (L3 and L4) showed high B factors and weak electron density, consistent with this region being rather unrestrained by DNA contacts in the locked structure. Minor changes also occur in the orientations of the side chains of residues in α4 that interact directly with C(6), particularly Ile79, Phe140 and His144, but they are generally rather subtle, and they suggest that the cytosine recognition pocket pre-exists on the surface of Tus awaiting the action of DnaB to liberate the C(6) base from the duplex. The imidazole side chain of His144 rotates upon the interaction of its $N^{\delta}H$ atom with C(6), bringing $N^{\varepsilon}H$ close enough to form a new hydrogen bond with the 5′-phosphate of T(8). It appears therefore that His144 exists as its conjugate acid in the locked complex.

Sequence Conservation and Mutants of Tus

The Tus-*Ter* replication termination system occurs infrequently among bacterial species, but Tus sequences are highly conserved in those species that have it (Neylon et al., 2005). Of the amino acid residues important for

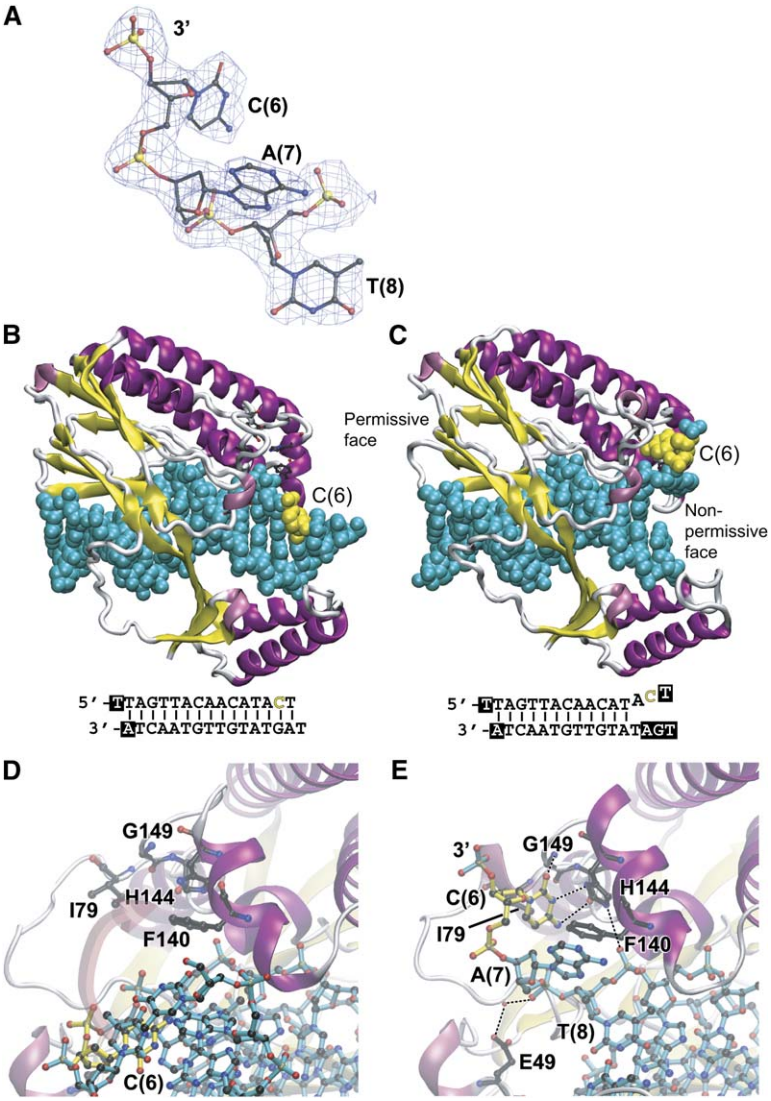

Figure 5. Structure of the Tus-*Ter* Lock

(A) Portion of the final $2F_o-F_c$ electron density map, contoured at 1 σ, showing the region of the displaced strand in the Tus-*Ter* lock complex. Comparison of structures of complexes of Tus with (B) wild-type *TerA* (PDB code 1ECR; Kamada et al., 1996) and with (C) an oligonucleotide with a forked structure at the nonpermissive face (PDB code: 2EWJ). The DNA molecules are shown in cyan in a space-filling representation, with the C(6) residue highlighted in yellow. Sequences of the oligonucleotides used for crystallization are shown below. Nucleotides shown in boxes are those that were not visible in the structures of the complexes.

(D) Structure of the DNA binding site at the nonpermissive face in the wild-type complex, showing the movement of C(6) required to form the locked structure, as displayed in (E). The figure was drawn using VMD (Humphrey et al., 1996).

Tus-*Ter* lock formation, Phe140, His144, and Gly149 are strictly conserved. Ile79 is conservatively substituted by Leu in some *Yersinia* species, and Leu150 by Val in some plasmid-encoded Tus variants.

A large number of mutants of Tus that are defective in function have been isolated from genetic screens, and some further mutants have been deliberately generated to test aspects of mechanism. With the exception of the E49K mutant, all of these have phenotypes that may be explained, either in terms of a direct effect on Tus-*Ter* interaction or an indirect effect on the folding of the protein (summarized in Neylon et al., 2005). The E49K mutant has little effect on the kinetic or thermodynamic properties of the Tus-*TerB* interaction, but is partially defective in anti-helicase activity in vitro, fork arrest in vivo, and interaction with DnaB (Skokotas et al., 1995; Mulugu et al., 2001). The crystal structure of the Tus-*Ter* lock shows that Glu49 of Tus makes a water-mediated hydrogen bond with the 5′-phosphate of the displaced A(7) nucleotide residue, and it would thus be expected to be partially defective in formation of the locked species.

To confirm the importance of residues in Tus that interact with C(6) or A(7) in the crystal structure of the locked complex (Figure 5) in stabilizing the complex with the forked oligonucleotides in solution, we used SPR to study the properties of E49A, I79A, F140A, and H144A mutants of Tus. Half-lives for dissociation of these proteins from oligonucleotides *TerB* and F5-*TerB*(wt) were compared with values for wild-type Tus (139 and 5300 s, respectively, Figure 3A). For Tus-E49A, half-lives of both complexes were decreased by a similar factor (to 82 and 3200 s, respectively), indicating a modest effect on the stability of both. For Tus-I79A, dissociation from the *TerB* complex was hardly affected (half-life of 141 s), but the half-life of the complex with F5-*TerB*(wt) was decreased about 9-fold to 560 s. As expected, the H144A mutation totally abrogated lock formation (half-life of 29 s) while reducing the half-life of the *TerB* complex to a similar value (23 s). These

data confirm the involvement of Ile79 and His144 in the formation of the locked structure. The results with Tus-F140A were most revealing. The half-life of the complex with the forked F5-*TerB*(wt) oligonucleotide was decreased, as expected, by 18-fold to 296 s. However, the complex with *TerB* was *stabilized* 10-fold (half-life of 1410 s). It is thus clear that if evolution were acting to select mutants of Tus with greater avidity for native *TerB*, as would be expected if strength of binding were the primary consideration, there would be no reason to conserve the side chain of Phe140. Its conservation clearly implicates the locking mechanism as being necessary for fork arrest in vivo.

Progress of the Helicase Leading to Lock Formation

The SPR data in Figure 3 and the availability of the two Tus-*Ter* structures allow us to chart the effects, in thermodynamic and kinetic terms, of progressive strand separation upon the entry of DnaB into the nonpermissive end of the Tus-*TerB* complex. Strand separation as far as A-T(4) (data for oligonucleotides F3n-*TerB* and F3n-*rTerB*) results in a slight weakening of the Tus-*TerB* interaction corresponding to a ~5-fold increase in K_D ($\Delta\Delta G$ ~0.9 kcal/mol). This is consistent with the loss of a single protein-DNA contact near the nonpermissive face, which, although affecting the strength of the interaction, does not change the rate of dissociation of Tus. The lack of strand specificity or effect of deletion of either strand (data for Δ3n-*TerB*, Δ3n-*rTerB*) suggests that this represents loss of an electrostatic interaction with the duplex DNA when the strands are separated. Lysine residues 192 or 195 of Tus may be involved in this, but since they are beyond the reach of the truncated *Ter* fragments in the crystal structures, we cannot comment further. Separation of the next base pair, A-T(5), has no further effect on the Tus-*TerB* interaction. Arg198 of Tus interacts with A(5) (and also G[6]) in the structure with duplex *TerA*, but most of its contribution to DNA binding is electrostatic or via interactions with the deoxyribose moieties (Neylon et al., 2000, 2005). This is consistent with there being no strand specificity with the forked DNAs, F4n-*TerB* and F4n-*rTerB* (Figure 3A). The Arg198 interactions may persist upon separation of the A-T(5) base pair but are not significant in the locked structure since complete removal of this strand (top strand in Figure 3A) had little effect on K_D (data for Δ5n-*rTerB* cf. F5n-*rTerB*).

With wild-type *TerB*, strand separation to G-C(6) produces the locked conformation (F5n-*rTerB*). Mutagenesis of T(5) to G in the locked oligonucleotide (i.e., F5-*TerB*[G5]) or its complete removal (in "single O/H C") increase K_D about 4-fold ($\Delta\Delta G$ ~0.8 kcal/mol). This suggests there might be some weak specific interaction of Tus with T(5), but it is not apparent in the crystal structure at 2.7 Å resolution. Mutagenesis of the critical C(6) residue to G (in F5n-*TerB*), A (in F5-*TerB*[A6]) or T (in F5-*TerB*[T6]) results in a consistent ~50-fold increase in K_D of the lock, indicating that the hydrogen bonds between the C(6) base and its binding residues in α4 of Tus contribute about 2.3 kcal/mol to the free energy of binding.

Two further questions remain, one which concerns the helicase specificity of replication fork arrest and the other, the mechanism of the unlocking of Tus from the arrested complex on subsequent approach of a second replication fork from the permissive face.

Helicase Specificity of Replication Fork Arrest

The ring-shaped replicative helicases like DnaB are at the forefront of the replisome, where they translocate in the 5′–3′ direction on the lagging strand template (Schaeffer et al., 2005). This strand passes through the center of the ring, while the leading strand template is sterically excluded at the front of the helicase molecule but not otherwise contacted in any specific way (reviewed in Patel and Picha, 2000; Neylon et al., 2005). The mechanism described here to explain polarity of fork arrest has clearly evolved to specifically block 5′–3′ ring helicases: the strand they displace is the one that contains the C(6) nucleotide of *Ter* that interacts with the cryptic cytosine-specific site in helix α4 of Tus to form the lock.

There is good evidence that the Tus-*Ter* complex can arrest DnaB in a polar manner, as assessed by orientation-dependent inhibition of in vitro strand-displacement assays (Lee et al., 1989; Khatri et al., 1989; Lee and Kornberg, 1992). There is also evidence, albeit sometimes contradictory (as discussed in detail in Neylon et al., 2005), that the progress of RNA polymerase and other helicases, including some that translocate in the 3′–5′ direction like Rep, PriA, UvrD, and SV40 T antigen, can be arrested at the nonpermissive face of the Tus-*Ter* complex. The structures of RNA polymerase and some of these (or related) helicases in complex with DNA templates are known (see, e.g., Korolev et al., 1997; Velankar et al., 1999; Murakami and Darst, 2003), and they show that strand separation occurs within the protein in a manner that would not give the C(6) base of *Ter* access to its locking site until the helicase had progressed far enough to completely displace Tus.

Data in Figure 3G and Table 1 may indicate that formation of the locked species is not strictly necessary to block helicase activities in a polar manner under conditions where they are usually measured, i.e., at low ionic strength or in potassium glutamate buffers. In contrast with the effects of forks at the permissive face (Figure 2A), strand separation as far into the complex as A-T(5) at the nonpermissive end is not itself sufficient to rapidly dissociate the Tus-*TerB* complex (Figure 3A). Persistence of the strong Tus-*Ter* interaction beyond unwinding of A-T(5) may thus account for its ability to exert a general polar block to the actions of helicases in vitro. Nevertheless, sufficient unwinding by DnaB to cause rapid dissociation of Tus, i.e., beyond G-C(6), necessarily allows the opportunity for the lock to form, and this would securely trap the replication fork.

Unlocking the Tus-*Ter* Lock

The last question concerns events in the last stage of chromosomal replication, when the later-arriving replication fork approaches the permissive face of a Tus-*Ter* complex at which the first-arriving fork is already stalled.

Events at this stage are not yet understood, but removal of Tus is clearly required to allow replication of the *Ter* site.

Is strand separation by DnaB at the permissive face now sufficient to unlock the locked complex? To probe this question, we measured rates of dissociation of Tus from doubly-forked *Ter* oligonucleotides with the lock sequence at the nonpermissive end (Figure 4C). As the forked regions were progressively lengthened at the other (permissive) end, the dissociation rates increased progressively, indicating that DnaB-mediated strand separation is sufficient even in this context to force dissociation of Tus. There appeared to be no special strand- or nucleotide-specific mechanism for this, suggesting as before that it is the progressive loss of contacts between the duplex DNA and Tus that forces its dissociation, rather than the existence of a specific unlocking mechanism.

EXPERIMENTAL PROCEDURES

Proteins and Oligonucleotides

Mutant derivatives E49A, I79A, and F140A of N-terminally His_6-tagged Tus were prepared following oligonucleotide-directed mutagenesis of the *tus* gene in the T7-promoter plasmid pCM862 (Neylon et al., 2000) using the QuikChange kit (Stratagene). The H144A mutation was introduced by polymerase chain reaction-based strand overlap extension (Neylon, 2004). All mutations were verified by nucleotide sequence determination. Tus, His_6-Tus, and mutant derivatives were prepared as described (Neylon et al., 2000); their concentrations were determined spectrophotometrically (ε_{280} = 39,700 $M^{-1}cm^{-1}$). Oligonucleotides, some of which (as specified) were modified at the 5′ end by a biotin residue followed by a 10-mer abasic poly(deoxyribose-5′-phosphate) spacer, were from GeneWorks (Adelaide, Australia); sequences of oligonucleotides are given in Figure S1.

SPR

Before use, aliquots of His_6-Tus were freshly diluted into SPR buffer (50 mM Tris.HCl at pH 7.5, containing 0.25 M KCl, 0.1 mM EDTA, 0.1 mM dithiothreitol, and 0.005% surfactant P-20). Measurements were carried out at 20°C using a Biacore 2000 instrument (Biacore AB, Uppsala, Sweden), essentially as described by Neylon et al. (2000). Two flow cells contained similar amounts of forked duplexes immobilized via one of the two 5′-biotinylated wild-type *TerB* strands, while the third flow cell contained fully double-stranded *TerB* (positive control), and the fourth was underivatized (blank). The amount of oligonucleotide was sufficient to bind 25–50 response units (RU) of Tus at saturating concentrations. A flow rate of 40 μl/min (Neylon et al., 2000) was used for all measurements, with Tus at 5–10 different concentrations. Surfaces were regenerated as required with injections (1–2 min at 5 μl/min) of 50 mM NaOH in 1 M NaCl. This was sufficient to remove the annealed nonbiotinylated DNA strands along with any tightly bound Tus. To generate new DNA surfaces, partially complementary, nonbiotinylated DNA strands were annealed by injection of 20 μl of 1 μM solutions of single-stranded oligonucleotides in SPR buffer. Tus does not bind to single-stranded oligonucleotides under the conditions of these experiments (Neylon et al., 2000). When required, injection of 1 M $MgCl_2$ (2 min at 5 μl/min) was sufficient to remove only Tus, leaving the oligonucleotides undisturbed. When dissociation rates were fast, data were globally fit to a 1:1 Langmuir binding model using BIAEvaluation software (Biacore). When rates were slow (i.e., with the complex in the locked configuration), the association and dissociation phases were studied separately. Second-order association rate constants (k_a) were obtained as slopes of plots of pseudo-first-order rate constants (k_{obs}) versus concentration of Tus, and values of k_d were obtained directly by fitting to a first-order rate law.

Dissociation Rates of Tus-*Ter* Complexes in Solution

The half-lives of complexes of His_6-Tus with *TerB* oligonucleotides (Table 1) were measured essentially as described (Skokotas et al., 1995). ^{32}P-labeled *Ter* DNA (0.05 nM) was equilibrated with Tus (0.25 nM) at 25°C in 50 mM Tris.HCl at pH 7.5, containing 0.20 M potassium glutamate, 0.1 mM EDTA, 0.1 mM dithiothreitol, and 100 μg/ml bovine serum albumin (KG_{200} buffer). Unlabeled wild-type *TerB* oligonucleotide (5 nM) was added as a trap to bind dissociated Tus. Samples were removed periodically and applied to nitrocelloulose filters, which were washed with KG_{200} buffer, dried, and counted in a scintillation counter.

Structure Determination

HPLC-purified lock oligonucleotides (5′-TTAGTTACAACATACT and 5′-TGATATGTTGTAACTA) were combined at 0.3 mM each in 25 mM Bis-Tris at pH 6.2 containing 100 mM NaCl, 1 mM EDTA, and 1 mM dithiothreitol and annealed by slow cooling from 70°C. To this mixture (0.25 ml) was added Tus (0.25 ml at 0.25 mM, in 50 mM sodium phosphate, pH 6.8, containing 50 mM NaCl, 0.1 mM EDTA, and 1 mM dithiothreitol). After 5 min at 20°C, the complex was diluted to 5 ml with 10 mM Bis-Tris at pH 6.3, containing 1 mM EDTA and 1 mM dithiothreitol, and then concentrated to 0.5 ml using an Amicon Ultra 15 centrifugal filter (MWCO 10 kDa). Dilution and concentration steps were repeated three times.

This Tus-*Ter* lock complex was crystallized by vapor diffusion at 18°C from hanging drops in 24-well trays. Reservoir solution (1 ml) consisting of 50 mM Bis-Tris at pH 6.75, containing 13% PEG 3350 and 0.2 M NaI, was equilibrated with a hanging drop of 4 μl of the complex mixed with 4 μl of reservoir solution. Bipyramidal crystals appeared after a week, and they grew to a maximum size (0.2 × 0.2 × 0.4 mm) after 3 weeks. They diffracted X-rays to 3.5 Å. Diffraction quality was improved by transferring crystals to artificial mother liquors with progressively increasing PEG 3350 concentrations; [PEG] was increased in 2.5% steps to a final concentration of 35% over 4 min intervals, giving X-ray diffraction to 2.7 Å. Crystals were snap frozen at 100 K using an Oxford cryostream. X-ray data were collected using a MAR345 image plate detector and goniostat system (Marresearch) that utilizes Cu Kα X-rays (λ = 1.5418 Å) from a Rigaku RU-200 (80 mA, 48 kV) rotating-anode generator with 300 μm focus Osmic blue optics (MSC Rigaku). Diffraction data were integrated and scaled using the DENZO and SCALEPACK programs from the HKL suite (Otwinowski, 1993).

The structure was solved by molecular replacement using the MOLREP package (Vagin and Teplyakov, 1997) and the coordinates of the Tus-*TerA* complex (Kamada et al., 1996). It was revealed that the crystals were of the same space group as those obtained for the Tus-*TerA* complex ($P4_12_12$), and the molecular replacement solution corresponded to the highest peaks from rotation and translation functions (7.54 σ and 45.2 σ, respectively). Model building and refinements were carried out using O (Jones et al., 1991) and REFMAC5 (Murshudov et al., 1997), respectively. A randomly selected set of 5% of the reflections were used to calculate R_{free} factors and validate the refinement strategy.

Supplemental Data

Supplemental Data include X-ray data collection and refinement statistics (Table S1) and sequences of all oligonucleotides used for SPR experiments with complete kinetic and thermodynamic data (Figure S1), and these can be found with this article online at http://www.cell.com/cgi/content/full/125/7/1309/DC1/.

ACKNOWLEDGMENTS

We thank J.M. Guss (University of Sydney) for use of X-ray data collection facilities. This work was supported by the Australian Research Council.

Received: December 19, 2005
Revised: March 16, 2006
Accepted: April 26, 2006
Published: June 29, 2006

REFERENCES

Bedrosian, C.L., and Bastia, D. (1991). *Escherichia coli* replication terminator protein impedes simian virus 40 (SV40) DNA replication fork movement and SV40 large tumor antigen helicase activity *in vitro* at a prokaryotic terminus sequence. Proc. Natl. Acad. Sci. USA *88*, 2618–2622.

Cheng, X., and Roberts, R.J. (2001). AdoMet-dependent methylation, DNA methyltransferases and base flipping. Nucleic Acids Res. *29*, 3784–3795.

Coskun-Ari, F.F., and Hill, T.M. (1997). Sequence-specific interactions in the Tus-*Ter* complex and the effect of base pair substitutions on arrest of DNA replication in *Escherichia coli*. J. Biol. Chem. *272*, 26448–26456.

Coskun-Ari, F.F., Skokotas, A., Moe, G.R., and Hill, T.M. (1994). Biophysical characteristics of Tus, the replication arrest protein of *Escherichia coli*. J. Biol. Chem. *269*, 4027–4034.

Duggan, L.J., Asmann, P.T., Hill, T.M., and Gottlieb, P.A. (1996). Identification of a Tus protein segment that photo-cross-links with *TerB* DNA and elucidation of the role of certain thymine methyl groups in the Tus-*TerB* complex using halogenated uracil analogues. Biochemistry *35*, 15391–15396.

Gottlieb, P.A., Wu, S., Zhang, X., Tecklenburg, M., Kuempel, P., and Hill, T.M. (1992). Equilibrium, kinetic, and footprinting studies of the Tus-*Ter* protein-DNA interaction. J. Biol. Chem. *267*, 7434–7443.

Henderson, T.A., Nilles, A.F., Valjavec-Gratian, M., and Hill, T.M. (2001). Site-directed mutagenesis and phylogenetic comparisons of the *Escherichia coli* Tus protein: DNA-protein interactions alone can not account for Tus activity. Mol. Genet. Genomics *265*, 941–953.

Hidaka, M., Kobayashi, T., Takenaka, S., Takeya, H., and Horiuchi, T. (1989). Purification of a DNA replication terminus (*ter*) site-binding protein in *Escherichia coli* and identification of the structural gene. J. Biol. Chem. *264*, 21031–21037.

Hidaka, M., Kobayashi, T., Ishimi, Y., Seki, M., Enomoto, T., Abdel-Monem, M., and Horiuchi, T. (1992). Termination complex in *Escherichia coli* inhibits SV40 DNA replication *in vitro* by impeding the action of T antigen helicase. J. Biol. Chem. *267*, 5361–5365.

Hill, T.M. (1992). Arrest of bacterial DNA replication. Annu. Rev. Microbiol. *46*, 603–633.

Hill, T.M., Henson, J.M., and Kuempel, P.L. (1987). The terminus region of the *Escherichia coli* chromosome contains two separate loci that exhibit polar inhibition of replication. Proc. Natl. Acad. Sci. USA *84*, 1754–1758.

Hill, T.M., Tecklenburg, M.L., Pelletier, A.J., and Kuempel, P.L. (1989). *tus*, the trans-acting gene required for termination of DNA replication in *Escherichia coli*, encodes a DNA-binding protein. Proc. Natl. Acad. Sci. USA *86*, 1593–1597.

Humphrey, W., Dalke, A., and Schulten, K. (1996). VMD: visual molecular dynamics. J. Mol. Graph. *14*, 33–38.

Jones, T.A., Zou, J.Y., Cowan, S.W., and Kleldgaard, M. (1991). Improved methods for building protein models in electron density maps and the location of errors in these models. Acta Crystallogr. *A47*, 110–119.

Kamada, K., Horiuchi, T., Ohsumi, K., Shimamoto, N., and Morikawa, K. (1996). Structure of a replication-terminator protein complexed with DNA. Nature *383*, 598–603.

Khatri, G.S., MacAllister, T., Sista, P.R., and Bastia, D. (1989). The replication terminator protein of E. coli is a DNA sequence-specific contrahelicase. Cell *59*, 667–674.

Korolev, S., Hsieh, J., Gauss, G.H., Lohman, T.M., and Waksman, G. (1997). Major domain swiveling revealed by the crystal structures of complexes of E-coli Rep helicase bound to single-stranded DNA and ADP. Cell *90*, 635–647.

Lee, E.H., Kornberg, A., Hidaka, M., Kobayashi, T., and Horiuchi, T. (1989). *Escherichia coli* replication termination protein impedes the action of helicases. Proc. Natl. Acad. Sci. USA *86*, 9104–9108.

Lee, E.H., and Kornberg, A. (1992). Features of replication fork blockage by the *Escherichia coli* terminus-binding protein. J. Biol. Chem. *267*, 8778–8784.

Mohanty, B.K., Sahoo, T., and Bastia, D. (1998). Mechanistic studies on the impact of transcription on sequence-specific termination of DNA replication and vice versa. J. Biol. Chem. *273*, 3051–3059.

Mulugu, S., Potnis, A., Shamsuzzaman, Taylor, J., Alexander, K., and Bastia, D. (2001). Mechanism of termination of DNA replication of Escherichia coli involves helicase-contrahelicase interaction. Proc. Natl. Acad. Sci. USA *98*, 9569–9574.

Murakami, K.S., and Darst, S.A. (2003). Bacterial DNA polymerases: the wholo story. Curr. Opin. Struct. Biol. *13*, 31–39.

Murshudov, G.N., Vagin, A.A., and Dodson, E.J. (1997). Refinement of macromolecular structures by the maximum-likelihood method. Acta Crystallogr. *D53*, 240–255.

Neylon, C. (2004). Chemical and biochemical strategies for the randomization of protein encoding DNA sequences: library construction methods for directed evolution. Nucleic Acids Res. *32*, 1448–1459.

Neylon, C., Brown, S.E., Kralicek, A.V., Miles, C.S., Love, C.A., and Dixon, N.E. (2000). Interaction of the *Escherichia coli* replication terminator protein (Tus) with DNA: a model derived from DNA-binding studies of mutant proteins by surface plasmon resonance. Biochemistry *39*, 11989–11999.

Neylon, C., Kralicek, A.V., Hill, T.M., and Dixon, N.E. (2005). Replication termination in *Escherichia coli*: structure and anti-helicase activity of the Tus-*Ter* complex. Microbiol. Mol. Biol. Rev. *69*, 501–526.

Otwinowski, Z. (1993). Oscillation data reduction program. In Proceedings of the CCP4 Study Weekend, 29–30 January 1993, L. Sawyer, N. Isaacs, and S. Bailey, eds. (Warrington, UK: Daresbury Laboratory), pp. 56–62.

Patel, S.S., and Picha, K.M. (2000). Structure and function of hexameric helicases. Annu. Rev. Biochem. *69*, 651–697.

Record, M.T., Jr., Ha, J.-H., and Fisher, M.A. (1991). Analysis of equilibrium and kinetic measurements to determine thermodynamic origins of stability and specificity and mechanism of formation of site-specific complexes between proteins and helical DNA. Methods Enzymol. *208*, 291–343.

Sahoo, T., Mohanty, B.K., Lobert, M., Manna, A.C., and Bastia, D. (1995). The contrahelicase activities of the replication terminator proteins of *Escherichia coli* and *Bacillus subtilis* are helicase-specific and impede both helicase translocation and authentic DNA unwinding. J. Biol. Chem. *270*, 29138–29144.

Schaeffer, P.M., Headlam, M.J., and Dixon, N.E. (2005). Protein-protein interactions in the eubacterial replisome. IUBMB Life *57*, 5–12.

Skokotas, A., Hiasa, H., Marians, K.J., O'Donnell, L., and Hill, T.M. (1995). Mutations in the *Escherichia coli* Tus protein define a domain positioned close to the DNA in the Tus-*Ter* complex. J. Biol. Chem. *270*, 30941–30948.

Vagin, A., and Teplyakov, A. (1997). *MOLREP*: an automated program for molecular replacement. J. Appl. Crystallogr. *30*, 1022–1025.

Velankar, S.S., Soultanas, P., Dillingham, M.S., Subramanya, H.S., and Wigley, D.B. (1999). Crystal structures of complexes of PcrA DNA helicase with a DNA substrate indicate an inchworm mechanism. Cell *97*, 75–84.

Accession Numbers

Coordinates for the crystal structure of the locked form of the Tus-*Ter* complex have been deposited in the Protein Data Bank under code 2EWJ.